Soft Matter

PAPER

View Article Online
View Journal | View Issue

Cite this: *Soft Matter*, 2014, **10**, 5532

Electrolytes based on alkoxysilyl-functionalized ionic liquids: viscoelastic properties and conductivity

L. Slemenik Perše,* M. Čolović, M. Hajzeri, B. Orel and A. Šurca Vuk

Received 4th April 2014
Accepted 19th May 2014

DOI: 10.1039/c4sm00752b

www.rsc.org/softmatter

Ionic liquids can be successfully used as electrolytes in electrochemical devices when they are in their quasi-solid state. Among several methods of solidification, a sol–gel process was chosen and a set of alkoxysilyl-functionalized iodide imidazolium-based ionic liquids were synthesized. The electrolytes were prepared by mixing these ionic liquids with a non-polymerisable ionic liquid (1-methyl-3-propylimidazolium iodide ($MPIm^+I^-$)). Iodine was dissolved in an electrolyte matrix in order to form an I_3^-/I^- redox couple. The change of the structure from sol to gel was followed by rheological tests in order to show the effect of different rheological parameters on the gelation process. The solvolysis with glacial acetic acid and condensation were followed by rheological experiments on the samples taken from a batch, and *in situ* on the rheometer. The formed three-dimensional sol–gel networks of various alkoxysilyl-functionalized ionic liquids differed in their microstructures and viscoelastic properties that were correlated with conductivity. The results show that the conductivity of approximately 10^{-3} S cm^{-1} at room temperature was achieved for the gels with relatively high values of elastic modulus and noticeable viscous contribution. It is shown that not only the viscosity but also the viscoelastic behavior and especially the relationship between viscous and elastic moduli (phase shift) together with the time of gelation are essential for the high conductivity of electrolytes.

1 Introduction

The interest in ionic liquids (ILs) has increased rapidly in recent years due to their unique properties, such as negligible vapor pressure, non-flammability, high ionic conductivity and electrochemical stability. ILs can be used in several applications as well as in redox electrolytes for hybrid electrochromic devices[1,2] and dye-sensitized photoelectrochemical solar cells (DSPECs).[3,4] The redox character of electrolytes is typically achieved *via* the presence of an I_3^-/I^- redox couple and can also be applied in hybrid electrochromic devices.[1,2,5]

A reliable electrochemical device requires electrolytes that combine high ionic conductivity ($\sigma > 10^{-4}$ S cm^{-1}) and mechanical stability with chemical, thermal, electrochemical stability, and compatibility with electrode materials.[3,6] The use of ILs is one of the promising ways for the preparation of electrolytes that would meet the above requirements. However, due to their fluid-like properties under ambient conditions, their application as electrolytes is limited (leakage, sealing costs, and reaction with sealing materials).[3,7,8] The prepared electrolytes should therefore be solidified and used in their quasi-solid state. Different approaches to solidification have been employed to date, *e.g.*, *in situ* polymerization of monomers in ILs,[9] confinement of ILs into silica networks,[10] and solidification with gelling agents (low-molecular weight gelators,[11] nanotubes,[12] and nanoparticles[13,14]). One possible method is the synthesis of polymerizable ILs, in which either the cation or the anion is functionalized with a polymerizable organic group, such as vinyl,[8,15,16] or methylacrylate.[8] Following this approach, our group started with the preparation of I_3^-/I^- redox electrolytes based on alkoxysilyl-functionalized ILs through the synthesis of single end-capped IL 1-methyl-3-[3-(trimethoxysilyl)-propyl]imidazolium iodide [$MTMSIm^+I^-$].[17–19]

After hydrolysis and condensation, the initial sol became highly viscous, enabling its application in DSPECs with a cell efficiency of 3.1%.[20] The additional functionalization of the $MTMSIm^+I^-$ [17–19] IL with short poly(ethylene oxide) (PEO) chains[22] due to the presence of more polar groups resulted in high solubility of LiI salt.[1] Iodide salts have often been added to redox electrolytes in DSPECs to increase photocurrents,[3,11,21,23,24] but in hybrid EC devices such salts are crucial for functioning, *i.e.*, the intercalation/deintercalation of small cations (Li^+) in/from the optically active WO_3 film. The as-prepared alkoxysilyl-functionalized IL 1-(2-(2-methoxyethoxy)ethoxy)ethyl-3-(3-(trimethoxysilyl)propyl)imidazolium iodide (single-$(EO)_2$)[1] (Fig. 1A) enabled high efficiency of hybrid EC devices (more than 4200 coloring/bleaching cycles, optical change in transmittance more than 45%). Due to the single end-capped nature of this IL, the condensed material at room temperature became highly

National Institute of Chemistry, Ljubljana, Slovenia. E-mail: lidija.slemenik.perse@ki.si

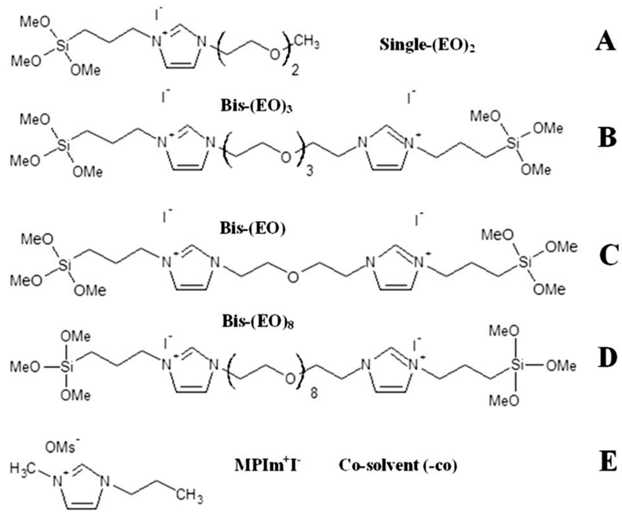

Fig. 1 Structures of alkoxysilyl-functionalized IL.

viscous and liquid-like, raising questions regarding the extent of sol–gel condensation and eventual formation of a soft solid-like material (gel).

The formation of a gel structure has often been followed by IR absorbance spectroscopy.[17–19,25] This powerful technique enables the study of solvolysis of sol–gel processes through the extinction of alkoxy bands, the formation of silyl ester bands of acetic acid and alkyl acetates, the eventual formation of a silanol ν(Si-OH) band at $\sim$910 cm^{-1} and the blue shift of modes in the siloxane region (1200–1000 cm^{-1}).[17–19,25] The differences in IR spectra can be correlated with the structure of the developing sol–gel matrix[17–19,25] and confirmed by independent techniques, such as ^{29}Si NMR spectroscopy.[1,18,19,26] Nevertheless, the indistinctiveness in the assignment of IR modes could occur when complex mixtures are considered.

Liquid-to-solid transition, independent of its nature, *i.e.* physical or chemical, represents a change in the mobility of the polymer matrix, and the formed gels exhibit different mechanical and rheological properties compared to the initial sols.[27–29] Changes in the rheological behaviour during the sol–gel process can therefore yield another independent and precise insight into gelation, and can precisely predict the gelation time and structural relationships during the process, especially when the rheological properties are followed *in situ*. The formed gel structure exhibits viscoelastic properties, resulting in either soft and elastic or hard and brittle material. Several publications can be found in the relevant literature regarding the determination of the gel point or the characterization of the viscoelastic properties of gels. There are studies devoted to sol–gel inorganic networks obtained from transition metal alkoxides[30] and tetraethoxysilane.[31] The rheological properties of organic–inorganic hybrid materials have become a matter of interest due to their dependence on the length of polymeric chains between alkoxysilyl reactive groups in bis end-capped hybrids[32] or dependence on the organic functionality in single end-capped hybrids.[17]

Nevertheless, only a few papers dealing with the rheological properties of electrolytes are mainly employed with lithium conductive electrolytes.[6,33,34] The viscosity/conductivity relationship was, for example, used to estimate the extent of ion pairing in electrolytes of sodium triflate and lithium perchlorate in poly(propylene oxide) electrolytes using the Walden plots, *i.e.* equivalent conductivity *vs.* shear viscosity.[33] Moreover, the viscosity–temperature relationship has been established for similar electrolytes on the basis of poly(propylene oxide).[34] More recently, studies of lithium trifluoromethanesulfonate containing a PEO polymer electrolyte have shown that different phases are characterized by distinct viscoelastic signatures; however, a direct correlation of rheological properties with conductivity was not made.[6] Even less can be found on the effect of rheological properties on the characteristics of electrolytes on the basis of ILs.[13,35,36] Direct correlation between viscosity and conductivity has been made for a series of low-melting ILs based on small aliphatic quaternary ammonium cations and imide anions.[35] It was stated that ionic conductivities are mainly governed by the viscosity and molar concentration of ILs. Dissolution of lithium salt decreased the conductivity, which was partly ascribed to the increase in viscosity, but this alone could not explain the change in conductivity.[35]

Despite the fact that diffusion constants of I_3^- ions in redox electrolytes and consequently the efficiency of DSPECs depend on the viscosity, rheological characterization has not been often considered. This is surprising since it has been shown for liquid electrolytes composed of 2,3-dimethyl-1-propylimidazolium iodide, LiI and I_2 in various organic solvents that increase in viscosity from 0.33 to 3.30 cPa decreased the short-circuit photocurrent density to almost half of their value.[23] ILs based on 1,3-dialkylimidazolium iodides have often been considered to be highly viscous in the literature, suggesting that their viscosity limits their use due to transport limitations.[37] Another approach, *i.e.* lowering of the viscosity of the 1-methyl-3-propylimidazolium iodide ($MPIm^+I^-$)/iodine electrolyte with the addition of low viscosity 1-ethyl-3-methylimidazolium dicyanamide, has been used to correlate the viscosity and the diffusion coefficient of I_3^- ions.[38] It has been shown that the I_3^- diffusion coefficients increased with decreasing $MPIm^+I^-$ concentration or increasing temperature, in both cases being related to decreased electrolyte viscosity. In the case of polymerizable ILs, the viscosities significantly increase during solidification. The aforementioned alkoxysilyl-functionalized IL $MTMSIm^+I^-$ [18] reveals a clear correlation between conductivity decrease and viscosity increase during the processes of hydrolysis (0.1 M HCl) and condensation. In quasi-solid electrolytes, the charge transport *via* diffusion of molecules remains important, but high concentrations of iodine lead to the formation of polyiodides and consequently to the transport of charge *via* the Grotthuss mechanism.[3,24,39]

With regard to the above facts, we decided to synthesize a series of single and bis end-capped alkoxysilyl-functionalized ILs (Fig. 1) for the preparation of redox I_3^-/I^- electrolytes. In addition to the aforementioned single end-capped IL (single-$(EO)_2$), three bis end-capped ILs, characterized by 1, 3 and 8 repeatable units between terminating alkoxysilyl groups, were prepared. The gelation of I_3^-/I^- redox electrolytes after the addition of the glacial acetic acid catalyst to different alkoxysilyl-functionalized ILs (Fig. 1) was followed using IR spectroscopy and various rheological tests. The goal of our study was to correlate structural changes during gelation obtained by dynamic rheological techniques with the conductivity of the electrolytes. To avoid the brittle character of gels, the non-reactive IL 1-methyl-3-propylimidazolium iodide ($MPIm^+I^-$) was applied as a co-solvent. The progress of the sol–gel process was characterized by viscoelastic properties, which were fitted using a five-parameter logistic model.[40]

2 Experimental

2.1 Preparation of sols

Synthesis of the single end-capped IL 1-(2-(2-methoxyethoxy)-ethoxy)ethyl-3-(3-(trimethoxysilyl)propyl)imidazolium iodide (single-$(EO)_2$) is reported in ref. 1. Briefly, a good alkylation reagent diethyleneglycol monomethylether monomesylate was used for monoalkylation of imidazole. The obtained 1-[2-(2-methoxyethoxy)ethyl]-1*H*-imidazole reacted with 2-iodopropyl-trimethoxysilane, which was used to introduce alkoxysilane groups (dialkylation) in position 3 of imidazole to obtain the single-$(EO)_2$ IL.[41] In the synthesis of bis end-capped ILs, two equivalents of imidazolium were used per one equivalent of the alkylation reagent. The same rule was taken into account in the dialkylation step with 3-iodopropyltrimethoxysilane.[41] In this way, the following ionic liquids were prepared (Fig. 1): 1,12-bis(3-(3-(trimethoxysilyl)propyl)imidazolium-1-il)-3-oxapentan diiodide (bis-(EO)), 1,14-bis(3-(3-(trimethoxysilyl)propyl)imidazolium-1-il)-3,6,9-trioxaundecan diiodide (bis-$(EO)_3$) and 1,29-bis(3-(3-(trimethoxysilyl)propyl)imidazole-1-il)-3,6,9,12,15,18,21,24-octaoxahexacosan diiodide (bis-$(EO)_8$).

Different alkoxysilyl-functionalized iodide ILs were used for the preparation of redox I_3^-/I^- electrolytes. Two redox electrolytes were prepared by dissolving 0.1 mol I_2 in 1 mol of single end-capped (single-$(EO)_2$) or bis end-capped (bis-$(EO)_3$) IL. The sol–gel process of solvolysis was initiated by the addition of glacial AcOH in a molar ratio of single-$(EO)_2$: AcOH = 1 : 3 and bis-$(EO)_3$: AcOH = 1 : 6. Three other electrolytes were prepared *via* the addition of IL 1-methyl-3-propylimidazolium iodide ($MPIm^+I^-$) as a co-solvent. Therefore, bis end-capped ILs were first mixed with the co-solvent in molar ratios of bis-(EO) : $MPIm^+I^-$ = 1 : 10, bis-$(EO)_3$: $MPIm^+I^-$ = 1 : 10 and bis-$(EO)_8$: $MPIm^+I^-$ = 1 : 30. The higher amount of co-solvent was added in the case of ILs with eight EO units to obtain an electrolyte with a similar initial viscosity value. After homogenization, I_2 (0.1 mol I_2/1 mol of alkoxysilyl-functionalized IL) was dissolved in order to form the I_3^-/I^- redox pair. Solvolysis and condensation were initiated by the addition of 6 mol of glacial AcOH per 1 mol of synthesized IL. Throughout the whole text the abbreviations indicating the structural characteristics of ILs (Fig. 1) are used to represent five different investigated electrolytes, comprising also the I_3^-/I^- redox pair, AcOH and eventually co-solvent ($MPIm^+I^-$).

2.2 Rheological measurements

The transition from sol to gel was followed continuously at a constant temperature (T = 23 °C), using small amplitude oscillatory tests at a constant frequency of oscillation ($\omega = 1$ Hz). A Physica MCR 301 controlled rate rheometer (Anton Paar) equipped with a cone-plate geometry sensor system (CP50/2°) was used for the rheological tests. The sensor system was protected with a special cover to avoid solvent evaporation during gelation.

Standard rotational flow tests were performed by a triangular method by changing the shear rate (0–1000–0 s^{-1}). Oscillatory stress sweep tests at a constant frequency of oscillation (1 Hz) were performed in order to determine the linear viscoelastic range (LVR). Frequency tests were performed at constant small deformation in LVR by decreasing the frequency of oscillation (20–0.01 Hz).

2.3 Conductivity measurements

Conductivity measurements of the electrolytes were performed using an Autolab PGSTAT302N potentiostat/galvanostat equipped with an FRA module for measurement of electrochemical impedance spectroscopy. The electrolyte was placed in a Teflon cell between two Pt electrodes, and the frequency range of electrochemical impedance spectroscopy (EIS) measurements was set between 10^5 and 0.01 Hz. Ionic conductivity σ was calculated from:

$$\sigma = \frac{d}{RA} \tag{1}$$

where R is the resistance determined from impedance spectra, while d and A are the thickness and area of the sample between Pt electrodes, respectively.

3 Results and discussion

3.1 IR absorbance spectroscopy

IR spectra offer a tremendous wealth of information about the structural changes that occur in electrolytes during gelation.[17–19,25] However, the complexity of the electrolytes, encompassing various precursor molecules, may lead to the overlapping of different modes and consequently, some information is diminished. The results of our study showed that a large number of modes, also superimposed on each other, appeared in the IR absorbance spectra of the investigated I_3^-/I^- electrolytes prepared from alkoxysilyl-functionalized ILs (Fig. 2).

Two examples are shown, *i.e.* an electrolyte on the basis of the single end-capped IL (single-$(EO)_2$) (Fig. 2A) and an electrolyte prepared from the bis end-capped IL (bis-$(EO)_8$) and co-solvent $MPIm^+I^-$ (Fig. 2B). IR absorbance spectra were taken immediately after dissolution of I_2 and addition of glacial AcOH (marked as initial), and after the elapsing of the time needed for gelation as obtained from rheology measurements (see below). The spectra were normalized with respect to the band at 1562 cm^{-1}, which was assigned to the imidazolium ring in-plane asymmetric stretching in 1-alkyl-3-methylimidazolium tetrafluoroborates[42] and hexafluorophosphates[43] and, in 1-alkyl-3-methylimidazolium hexafluorophosphates, also to $CH_2(N)$ and $CH_3(N)$ stretching.[43]

The initial spectrum of the single-$(EO)_2$ electrolyte (Fig. 2A) clearly revealed the presence of the AcOH catalyst (marked with 'a') and the bands of IL (marked with '*'). Regarding the process

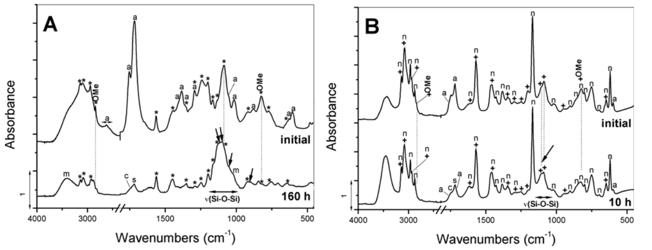

Fig. 2 IR absorbance spectra of the studied electrolytes before and after rheology testing: (A) single-$(EO)_2$ and (B) bis-$(EO)_8$-co. * denotes single-$(EO)_2$; + denotes bis-$(EO)_8$; n – co-solvent $MPIm^+I^-$; a – acetic acid; m – methanol; s – silyl ester of acetic acid; c – methylacetate; OMe – methoxysilyl groups. All compositions also contained I_2 to form the I_3^-/I^- redox pair and sol–gel catalyst, *i.e.* glacial AcOH.

of gelation, the most important characteristics of this spectrum were methoxy modes at 2840 and 820 cm^{-1},[1] while the other two methoxy bands (1196, 1094 cm^{-1}) were overlapped by the modes of imidazolium ring, $CH_2(N)$ and $CH_3(N)$ stretching.[42,43] After 160 h in a rheometer, the IR absorbance spectrum revealed a drastic decrease in the intensity of AcOH bands. The methoxy modes at 2840 and 820 cm^{-1} practically disappeared from the spectra, indicating that the solvolysis reaction, *i.e.* Si-OR + AcOH → Si-OAc + R-OH,[25,44] took place. The band at around 1720 cm^{-1} (marked with 's') was (in our previous work on methyltriethoxysilane[25]) tentatively assigned to the silyl ester of acetic acid (Si-OAc), due to its position between the acetic acid carbonyl (1712–1715 cm^{-1}) and the corresponding mode of ethylacetate (1740 cm^{-1}). In parallel, the mode of methylacetate can also be noted in the IR spectrum obtained after 160 h (Fig. 2A) as a shoulder band (marked with 'c'), since methylacetate can also be formed as a product of the esterification reaction between methanol (by-product of solvolysis) and AcOH or condensation between Si-OAc and Si-OR.[25,44]

In addition to some unreacted Si-OAc groups in the Si–O–Si network, a small amount of terminal Si-OH silanols might form as well, possibly leading to a low intensity ν(Si-OH) shoulder at 908 cm^{-1} (marked with an arrow). Water molecules, needed for the formation of silanol bands, could be formed in reactions of esterification with AcOH[25,44] or may enter the sol from the atmosphere during its preparation. The condensation to Si–O–Si linkages can be judged from the formation of new bands at 1115, 1100 and 1051 (shoulder) cm^{-1} in the siloxane spectral region (1200–1000 cm^{-1}). The other shoulder at 1030 cm^{-1}, together with the broad OH mode at 3410 cm^{-1}, might indicate the presence of a methanol by-product (marked with 'm') that remained trapped in the sample inside the sensor system of the rheometer. To conclude, the measured IR spectra enabled the conclusion that the newly formed bands in the siloxane region confirm the formation of siloxane linkages in the single-$(EO)_2$ electrolyte. However, due to the overlapping with the modes of the imidazolium ring, and $CH_2(N)$ and $CH_3(N)$ stretching,[42,43] the conclusions about the extent of the Si–O–Si linkages could not be unambiguous.

For the bis-$(EO)_8$-co redox electrolyte with a co-solvent (Fig. 2B), the bands indicative of sol–gel processes were even more blurred by the presence of the co-solvent. Since the molar ratio in ILs bis-$(EO)_8$-co was 1 : 30, the bands of the non-reactive $MPIm^+I^-$ co-solvent (marked with the letter 'n') dominated the spectrum (Fig. 2B). The methoxy mode of bis-$(EO)_8$ (marked with '+') could be noted as a weak shoulder in the initial spectrum, while the one at 820 cm^{-1} was superimposed on the band of the co-solvent. After 10 h of gelation, the methoxy mode at 2840 cm^{-1} disappeared from the spectrum, while the band at 820 cm^{-1} significantly decreased in intensity. These changes indicate that the solvolysis reaction took place. Some bands of AcOH could be noted in the initial spectrum, but decreased considerably after 10 h. The modes of the silyl ester of acetic acid and methylacetate can be observed instead. In the siloxane spectral region, the band at 1105 cm^{-1} increased in intensity relatively with regard to the band at 1091 cm^{-1}, which could be ascribed to the formation of the siloxane network. The extent of condensation to tridimensional gel, however, could not be judged, due to the overlapping of siloxane modes with the imidazolium ring in-plane asymmetric stretching and $CH_2(N)$ and $CH_3(N)$ stretching[42,43] of both ILs, *i.e.* the alkoxysilyl-functionalized bis-$(EO)_8$ and $MPIm^+I^-$ co-solvent. Due to the lack of information about the extent of the sol–gel process obtained with IR, the progression of the sol–gel process was followed by different rheological measurements.

3.2 Rheological characterization

3.2.1 *Ex situ* flow and frequency tests. Flow tests under destructive shear conditions were carried out at different times from the beginning of solvolysis. Fig. 3 shows that all initial electrolytes exhibited Newtonian flow behavior with low viscosity, depending on the IL used. The lowest initial viscosity was obtained for the electrolyte prepared from the single end-capped IL (0.037 Pa s, Fig. 3A), while the initial viscosity of the electrolyte, prepared from bis end-capped IL bis-$(EO)_3$, was 0.29 Pa s (Fig. 3B). Electrolytes with co-solvent $MPIm^+I^-$, which were also made from bis end-capped ILs, exhibited an initial viscosity of 0.20 Pa s and 0.21 Pa s for bis-$(EO)_3$-co and bis-(EO)-co, respectively (Fig. 3D and E). When the IL with longer poly(ethylene oxide) chains, *i.e.* bis-$(EO)_8$-co, was used, the initial viscosity of the electrolyte was the highest (0.35 Pa s, Fig. 3C) despite the fact that a larger amount of co-solvent was used. As solvolysis proceeded, the consistency of liquids started to increase, which was reflected in higher viscosity. For the single-$(EO)_2$ + I_2 + AcOH electrolyte, prepared from a single end-capped IL (Fig. 3A), the viscosity was Newtonian, *i.e.* independent of the shear rate, even 160 h after the beginning of solvolysis. In contrast, the flow behavior of electrolytes based on bis end-capped ILs changed to shear thinning after 2, 10, 15 or 20 h, indicating their ability to form tridimensional networks due to the presence of terminal alkoxysilyl groups at both ends of the IL. At the end of the sol–gel process, these electrolytes exhibited shear-thinning flow behavior, which was for bis-$(EO)_3$ + I_2 + AcOH (Fig. 3B) time-independent, while hysteresis, observed for flow curves of electrolytes with the co-solvent (Fig. 3C–E), implies the time-dependent thixotropic behavior of the formed gel structures. The increase of the viscosity with time for the

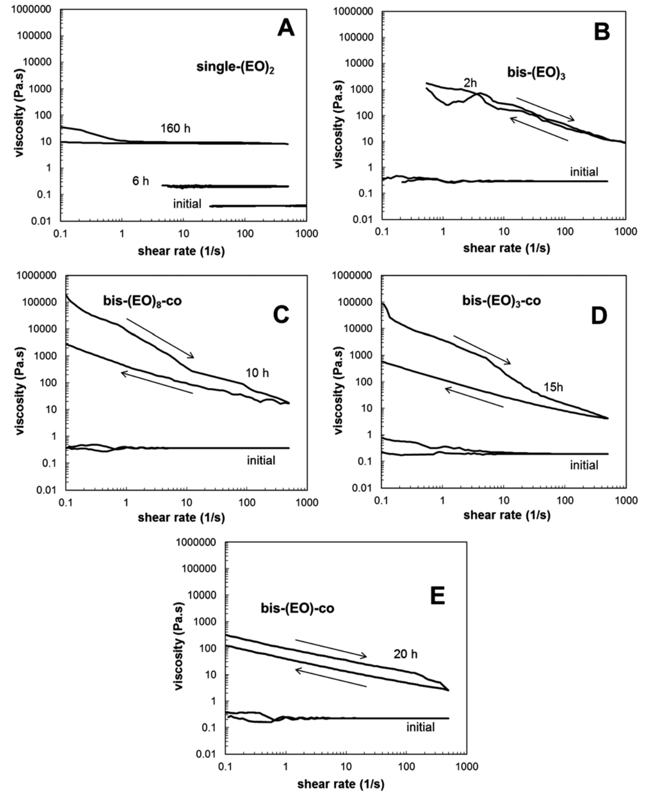

Fig. 3 Flow curves of IL-based electrolytes at the beginning and at the end of solvolysis. All compositions also contained I_2 to form the I_3^-/I^- redox pair and sol–gel catalyst, *i.e.* glacial AcOH.

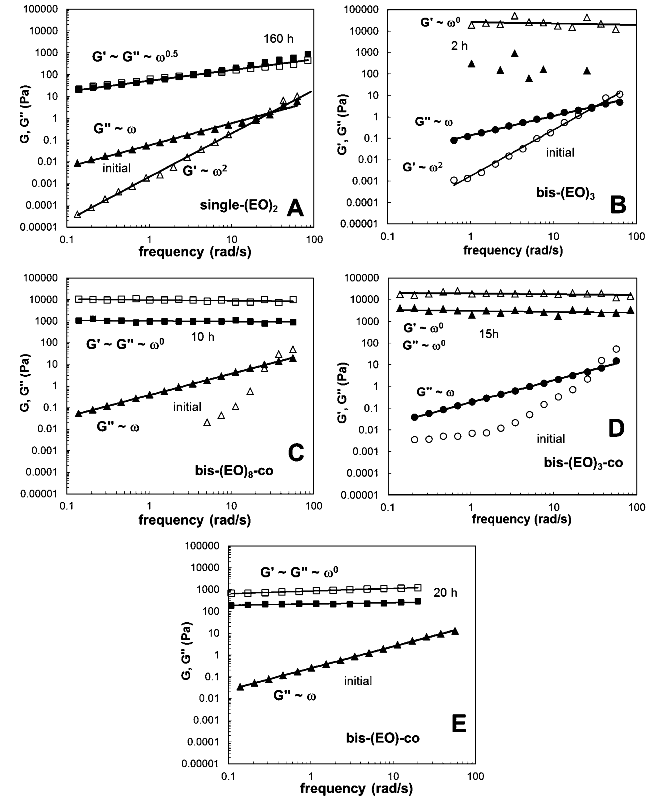

Fig. 4 Oscillation tests: frequency dependence of dynamic moduli G' and G'' for IL-based electrolytes at the beginning and at the end of sol–gel processes. All compositions also contained I_2 to form the I_3^-/I^- redox pair and sol–gel catalyst, *i.e.* glacial AcOH.

single-$(EO)_2$ + I_2 + AcOH electrolyte was slow, *i.e.* 160 h after the beginning of solvolysis the viscosity increased from initial 0.035 Pa s to ~10 Pa s (Fig. 3A). This is a consequence of the single end-capped character of this IL, preventing the formation of a firm tridimensional sol–gel network. However, the increase of the viscosity for other electrolytes was much faster with higher final viscosities (Fig. 3B–E).

The rheological properties of electrolytes were, at different times during the gelation process, followed by oscillation tests in the range of the linear viscoelastic response (Fig. 4). At the beginning, the initial electrolyte made of single end-capped IL (single-$(EO)_2$) (Fig. 4A) exhibited lower values of dynamic storage modulus G' compared to loss modulus G''; moreover, the moduli exhibited different dependences on the frequency of oscillation. The storage modulus was scaled with the frequency as $G' \sim \omega^2$, while G'' was linear in frequency ($G'' \sim \omega$). These are characteristics of the viscoelastic "liquid-like" behavior.[45] As the gelation proceeded, the values of the moduli increased and their dependences on the frequency changed; 160 h after the beginning of solvolysis, G' equaled G'', and both moduli depended on the frequency of oscillation by the order of 0.5. Such behavior is characteristic for weak gels, which resemble the strong gels in their mechanical behavior, particularly at low frequencies, but as the deformation increases, their networks undergo a progressive breakdown into smaller clusters. As a consequence, the system can flow with flow properties typical of a disperse system.[46] In contrast, sols based on bis end-capped IL precursors (Fig. 4B–E) exhibited "liquid-like" behavior with strong domination of viscous modulus G'' at the beginning, while completely different viscoelastic behavior was observed for the gels at the end of gelation. The formed gels exhibited a "solid-like" behavior with much higher values of the storage modulus G' compared to the loss modulus G''; moreover, the moduli were frequency independent, *i.e.* $G' \sim \omega^0$. Such behavior is characteristic for strong gels,[45] which are usually, due to the lack of viscous contribution, also very hard and brittle. Under the conditions of small deformation, strong gels manifest the typical behavior of viscoelastic solids and, above a critical deformation value, they rupture rather than flow.[45] For the bis-$(EO)_3$-based electrolyte without the co-solvent (Fig. 4B) the transition from sol to gel was completed in 2 h, while for other electrolytes with the co-solvent the structure of a strong gel was observed after 10, 15 and 20 h (Fig. 4C–E). The addition of an IL co-solvent obviously prolonged the time of gelation due to the larger distance between the precursor molecules after the beginning of solvolysis.

For chemical, *i.e.* covalently cross-linked, gels formed in our study, linear viscoelastic behavior has been extensively investigated in the vicinity of the sol–gel transition point. Winter and Chambon[27,47] showed that at the critical gel point dynamic moduli follow a simple power law: $G'(\omega) \approx G''(\omega) \sim \omega^n$, where n depends on the particular gelation mechanism. In our work, the transition from sol to gel was observed for the single end-capped-based electrolyte (Fig. 4A), where at 160 h the G' and G'' depended on the frequency by the order of 0.5 ($G' \sim G'' \sim \omega^{0.5}$).

3.2.2 *In situ* rheological time tests. More detailed and very reliable information about the sol-to-gel transition has been obtained by performing *in situ* rheological measurements (time tests, Fig. 5 and 6). These tests should be performed under non-destructive oscillatory conditions in the linear viscoelastic range, where the applied amplitude is small enough not to interfere with the microstructure or the mechanism of gelation. The advantage of these tests is a continuous observation of the evolution of viscoelastic properties as the sol goes through the gel point.

The results (Fig. 5) showed that at the beginning of the solvolysis all initial sols exhibited "liquid-like" behavior with low consistency and dominating viscous behavior, similar to that detected with frequency tests (Fig. 4). The loss modulus G'' was high, while the storage modulus G' was low or negligible. Furthermore, the loss modulus G'' increased continuously, while the storage modulus G' rose sharply until it intersected and exceeded the loss modulus. The time at which both moduli reached the same value indicated the sol–gel transition point, which is often referred to as a "gel-point".[48] From this point onward, the elastic behavior G' dominated and the behavior of the sample became "solid-like". Both moduli leveled off as the reaction came to completion. For the single-$(EO)_2$ + I_2 + AcOH system (Fig. 5A), the gel formed after ~115 h, followed by constant values of dynamic moduli ($G' \sim G''$) of ~250 Pa with a slight prevalence of G'. Such weak gel behavior could be understood as an intermediate between the properties typical of liquids (sols) and properties peculiar to strong gels. As already mentioned, single-$(EO)_2$ belongs to single end-capped compounds that, due to the presence of the alkoxysilyl terminating group on only one side of the precursor molecule, obstructs the formation of a firm interconnecting silica network. In contrast, gels with highly expressed storage modulus were detected for samples (Fig. 5B and C), based on bis end-capped ILs. Moreover, three electrolytes with the $MPIm^+I^-$ co-solvent (Fig. 5C) exhibited a noticeable loss modulus, a considerably long time after the gel-point, while the loss modulus for the bis-$(EO)_3$-based electrolyte without the co-solvent (Fig. 5B) dropped to zero immediately after the gel-point. For this electrolyte, the rheological properties indicated the formation of a strong and brittle gel.

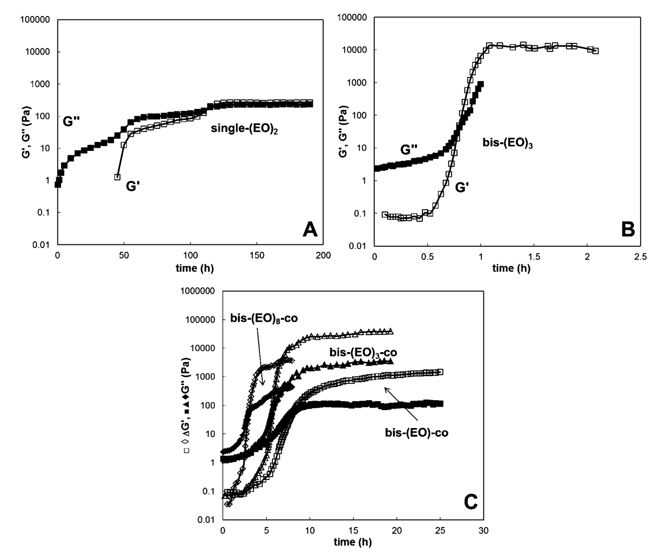

Fig. 5 Time course of the gelation process in the linear viscoelastic range for electrolytes based on ILs. All compositions also contained I_2 to form the I_3^-/I^- redox pair and sol–gel catalyst, *i.e.* glacial AcOH.

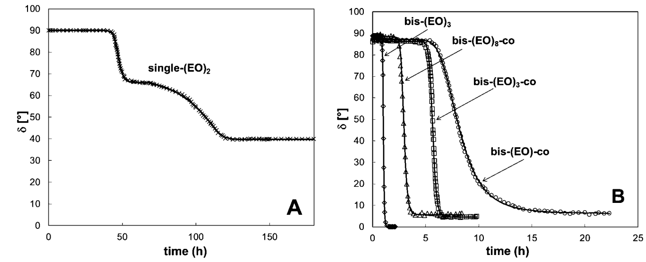

Fig. 6 Time dependence of the phase shift angle. Symbols represent experimentally determined values, while curves signify the fitted values obtained by a five-parameter logistic function (eqn (2)).

Another promising demonstration of the progression of the sol–gel process is the presentation of phase shift angle δ as a function of gelation time (Fig. 6A and B). The tan δ value is calculated as the quotient of the lost and stored deformation energy; it reveals the ratio of viscous and elastic contribution to viscoelastic behavior. In general, the ideal-elastic behavior, where G' completely dominates G'', is specified in terms of $\delta = 0$, while ideal-viscous behavior is expressed as $\delta = 90°$ since G'' completely dominates G'. δ equals 45° for materials where viscous and elastic contributions exactly balance (*i.e.* $G' = G''$).

The point when $\delta = 45°$ is an important analysis criterion for gel formation,[48] because it indicates the sol-to-gel transition point. For the IL samples used in our study, three different shapes of δ *vs.* t curves were observed (Fig. 6). The longest time of gelation and the gentlest decrease of δ from 90° (ideal viscous) towards lower values (gel state) were observed for the electrolyte based on the single end-capped IL (single-$(EO)_2$, Fig. 6A). δ reached the value of ~40° after 120 h of the gelation process and remained constant for another 60 h. At this time, the state of approximately balanced viscous and elastic portions of the viscoelastic behavior, typical of weak gels, was reached. Moreover, two steps of the gelation process can be determined for this electrolyte (Fig. 6A). At the first step, the δ value was constant (at 90°) for ~40 h; it then sharply decreased for ~10 h to intermediate $\delta \sim 65°$ where a second plateau was observed. The next step of the gelation process began with the decrease of δ from the second plateau value, which was slower, and the lowest value of $\delta \sim 40°$ was achieved after 70 h of decrease. The slow gelation process of this electrolyte led to the final weak gel, which could be applied in DSPECs or hybrid EC devices, enabling penetration into the pores of the electrode coatings and thus good contact.

For electrolytes based on bis end-capped precursors, a one-step gelation process and fast formation of gels were observed (Fig. 6B). The sharpest drop of δ, *i.e.* the fastest gelation, was observed for the bis-$(EO)_3$ + I_2 + AcOH electrolyte, which was also the only mixture for which δ reached the value of $\delta = 0°$, indicating a solid state rigid behavior of this gel. Electrolytes with 3 and 8 repeating units (Fig. 6B) showed a very similar sharp decrease of δ with the time of solvolysis. For both electrolytes, the curves were almost parallel; δ reached similar final values ($\delta \sim 5°$) of solvolysis, while the time needed to reach the final gel structure was not the same. The electrolyte based on IL bis-$(EO)_8$ with the co-solvent gelled in 5.7 h (Table 1), while the electrolyte on the basis of bis-$(EO)_3$ with the co-solvent gelled in 4.6 h. Different shapes of the δ *vs.* time were observed for the electrolyte bis-(EO)-co. The drop of δ from the initial value close to 90° was sharp at the beginning, while the approach to the lowest value at the end of the gelation process was slow and the shape of the curve was gentle (Fig. 6B). The asymmetry of this curve was the highest.

In order to evaluate and quantify the parameters important for the sol–gel process, the experimental asymmetric dependences of phase shift angle δ on the time of solvolysis were the best fitted with the five-parameter logistic function:[40]

$$\delta = \delta_{\max} - \frac{(\delta_{\max} - \delta_{\min})}{\left(1 + \left(\frac{t}{t_g}\right)^{-W}\right)^{s}} \tag{2}$$

where $\delta_{\max}$ and $\delta_{\min}$ are the highest (initial) and the lowest (the end) values of phase shift angle, respectively, t_g is the time of sol–gel transition, while s jointly with W controls the rate of approach to the $\delta_{\min}$ asymptote.

Due to the two-step gelation process, the curve of the single-$(EO)_2$ electrolyte was fitted with additional parameters. The results (Fig. 6) showed excellent agreement of the experimental data with the predicted values for all electrolytes used. The five-parameter logistic model enabled the exact determination of the time, at which the sol–gel transition occurred t_g together with precise viscoelastic properties of the formed gels δ_2. Moreover, the model can be used for accurate prediction of the total rate and time of the gelation process (W, s) of alkoxysilyl-functionalised IL-based electrolytes (Table 1).

3.3 Conductivity measurements

The redox I_3^-/I^- electrolytes studied in this work were prepared for their application in DSPECs and hybrid electrochromic devices. One of the objectives was to define the eventual correlation between rheological measurements and conductivity (Fig. 7). Similar to the rheological characterization (Fig. 3–6), three distinctive types of time-dependent curves were observed for conductivity values (Fig. 7).

The rheological properties of bis-$(EO)_3$ as the electrolyte with the most brittle and rigid gel structure were reflected in the lowest values of conductivity. Immediately after the addition of glacial AcOH, the conductivity of this electrolyte was 1.01×10^{-3} S cm^{-1}, but dropped to 5.1×10^{-6} S cm^{-1} after 10 h. The electrolyte on the basis of single end-capped IL single-$(EO)_2$ revealed an ionic conductivity of 1.82×10^{-3} S cm^{-1} at the beginning of solvolysis, while the conductivity decreased to a constant value of 1.1×10^{-4} S cm^{-1} during the formation of the weak gel. The electrolytes with co-solvents exhibited the highest values and similar time-dependent behavior of conductivities. After the addition of the sol–gel catalyst, the conductivity of these electrolytes varied between 2.4×10^{-3} and 2.6×10^{-3} S cm^{-1}; it then slowly increased to a stabilized value of 9.8×10^{-3} S cm^{-1} for bis-(EO)-co, 3.8×10^{-3} S cm^{-1} for bis-$(EO)_8$-co and 3.3×10^{-3} S cm^{-1} for the bis-$(EO)_3$-co electrolyte gel. The final values of conductivity regarding the type of electrolyte were in the same order as the final consistencies of electrolyte gels, obtained from rheological measurements (Fig. 5) ranging from 234, 1500 to 4340 Pa s for electrolytes made from precursors with 1, 8 and 3 EO units, respectively.

The bis-$(EO)_3$ + I_2 + AcOH gel with the lowest conductivity exhibited high mechanical stability with extremely high values of elastic modulus G' ($G' > 10^5$ Pa) and negligible viscous contribution ($\delta = 0°$). Such viscoelastic behavior indicates the presence of a three-dimensional network typical of strong gels. Due to the dense structure, the values of conductivity decreased significantly as a consequence of suppressed diffusion of I_3^- ions. Moreover, the quick formation of a compact siloxane network resulted in the inability of polyiodides to form charge carrier paths for Grotthuss-type transfer mechanisms. In contrast, the highest conductivity values were observed for the three electrolyte gels with the $MPIm^+I^-$ co-solvent characterized not only by a high elastic modulus but also noticeable viscous contribution ($\delta > 0°$). The sol-to-gel transition for these gels

Table 1 The parameters of the five-parameter logistic model (eqn (2)) for the investigated electrolytes

	Single-EO_2	Bis-EO_3	Bis-EO_8-co	Bis-EO_3-co	Bis-EO-co
$\delta_{\max1}$	90.0	88.8	89.1	86.3	87.0
$\delta_{\max2}$	67.5				
$\delta_{\min1}$	65.9	0.003	5.7	4.6	6.3
$\delta_{\min2}$	39.6				
t_{g1} (h)	46.3	1.0	2.9	5.6	6.5
t_{g2} (h)	112.1				
W_1	1.8	26.4	17.8	30.0	6.2
W_2	4.8				
S_1	1.5	1.19	1.17	1.18	3.1
S_2	0.12				

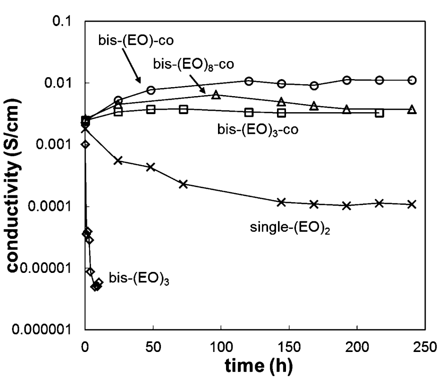

Fig. 7 Time-dependent conductivity measurements of redox electrolytes. All compositions also contained I_2 to form the I_3^-/I^- redox pair and sol–gel catalyst, *i.e.* glacial AcOH.

occurred in $t_g \sim 2.9$ to 6.5 h (Fig. 5 and Table 1), while t_g for two gels with lower conductivity and without co-solvents was either faster (1 h) or extremely slow (46.3 h). In the case of the single end-capped single-$(EO)_2$-based electrolyte, the formed network provided significant elastic as well as viscous contribution to the viscoelastic properties. The formed gel was soft and able to easily flow under shear, which is the consequence of the single end-capped character of the precursor IL. Due to the smaller consistency (viscosity) and lower mechanical stability, the diffusion of the formed I_3^- ions was most probably responsible for charge transfer and the measured conductivity stabilized at $\sim 1.1 \times 10^{-4}$ S cm^{-1} after approximately 160 h. Presumably, due to the soft gel structure and consequent relatively high mobility of the weakly bonded network, the conduction was most probably limited to the diffusion of ions.[3,24] In contrast, the electrolytes prepared from bis end-capped ILs and the $MPIm^+I^-$ co-solvent were characterized by strong gel-like viscoelastic properties. The gels provided high elastic contribution G' with noticeable viscous effects G''. The result was the highest conductivity of this type of gel, which might have arisen either from diffusion of I_3^- ions *via* a liquid co-solvent or also by establishing polyiodide paths for a Grotthuss-type transfer mechanism. The stabilized values of conductivities for these gels were obtained after 10–20 h, *i.e.* the time as measured to obtain gels with stable properties (Fig. 3).

We conclude that the rheological properties and conductivity of the formed solid-like electrolytes depend strongly on the chemical structure of functionalized ionic liquids, the addition of $MPIm^+I^-$ and the gelation time. Electrolytes based on the single end-capped ionic liquid (single-$(EO)_2$) exhibited a long gelation time and weak solid-like behaviour resulting in poor conductivity. On the other hand electrolytes based on the bis end-capped ionic liquid (bis-$(EO)_3$) exhibited solid-like properties with a lack of viscous contribution ($\delta \sim 0°$) resulting in fast gelation time and extremely low conductivity values. The addition of $MPIm^+I^-$ to bis end-capped ionic liquids (bis-$(EO)_8$-co, bis-$(EO)_3$-co, bis-(EO)-co) resulted in a moderate solvolysis time and viscoelastic solid-like properties with δ from 2.9° to 6.5°, which enabled the highest values of conductivity.

In order to achieve high conductivity values, the time of gelation is important, but viscoelastic properties, especially the value of elastic modulus G', and the presence of viscous contribution of the solid-like electrolyte are significant.

Finally, as a result of these findings, the stabilized conductivity values were compared to the elastic properties of the formed gels (Fig. 8). Interestingly, a good correlation between the conductivity and G' was obtained for the electrolytes prepared with the addition of co-solvent $MPIm^+I^-$, which also exhibited similar rheological properties and high conductivity values. Nevertheless, the results showed that the increase in G' (*i.e.* strong gel structure) exponentially decreased the values of conductivity.

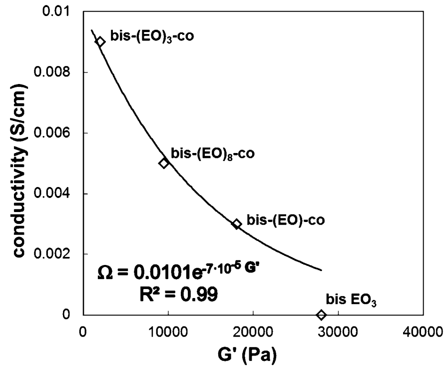

Fig. 8 Variation of conductivity with elastic contribution G' for gels, used in the study.

4 Conclusions

The study of the sol–gel process with rheological measurements has shown the great importance of viscoelastic properties for the high conductivity of electrolytes based on ILs. Rheological properties enabled an *in situ* study of the changes in the structure during transition from sol to gel. The dynamic measurements in the oscillatory mode showed that the initial sol state was characterized by $G' \sim \omega^2$ and $G'' \sim \omega$, while the formed gel structure showed $G' \sim G'' \sim \omega^0$ dependence. The intermediate gel point was characterized by the power-law dependence ($G' \sim G'' \sim \omega^{0.5}$) of both moduli on the frequency of oscillation.

It has been shown that not only the viscosity, but also the viscoelastic properties, *i.e.* elastic and viscous contribution, are particularly important factors responsible for good conductivity. The results have shown that high elasticity and the lack of viscous contribution lead to extremely dense structures resulting in decreased mobility and hence poor conductivity. Moreover, it has been shown that the conductivity of the formed gel structures could be correlated with viscoelastic properties, *i.e.* elastic contribution (G') of the gel. The *in situ* rheological measurements and fitting of the experimental results with a five-parameter logistic function enabled the precise determination of the time for sol–gel transition, the viscoelastic characteristics of the formed gel, and the rate of the sol–gel process. The fast gelation process of (bis-$(EO)_3$) led to a gel with a very dense network and rigid gel structure reflected in decreased conductivity. In contrast, a slow gelation process of the single-$(EO)_2$ based electrolyte resulted in a viscoelastic weak gel with sol–gel networks that can undergo a progressive breakdown as the deformation increases. The system can flow with flow properties typical of a disperse system and, due to the decreased viscosity, the mobility is increased and conductivities are higher. The highest values of conductivity, however, were achieved with gels exhibiting viscoelastic behavior with high elastic contribution and a noticeable viscous modulus at the end of solvolysis.

Acknowledgements

This research was supported by the European Community's Seventh Framework Programme (FP7) under Grant Agreement no. 200431 (Innoshade), Centre of Excellence Low-carbon Technologies and Slovenian Research Agency (Programme P1-

0030). Marija Čolović and Metka Hajzeri acknowledge the Slovenian Research Agency for their Ph.D. grants.

References

1 M. Čolović, A. Šurca Vuk, M. Hajzeri and B. Orel, *Mater. Res. Bull.*, 2012, **47**, 3160.
2 M. Čolović, I. Jerman, M. Gaberšček and B. Orel, *Sol. Energy Mater. Sol. Cells*, 2011, **95**, 3472.
3 A. Hagfeldt, G. Boschloo, L. Sun, L. Kloo and H. Pettersson, *Chem. Rev.*, 2010, **110**, 6595.
4 B. O'Regan and M. Grätzel, *Nature*, 1991, **353**, 737.
5 A. Georg and A. Georg, *Sol. Energy Mater. Sol. Cells*, 2009, **93**, 1329.
6 G. Zardalidis, E. Ioannou, S. Pespas and G. Floudas, *Macromolecules*, 2013, **46**, 2705.
7 I. Lee, S. Hwang and H. Kim, *Sol. Energy Mater. Sol. Cells*, 2011, **95**, 315–317.
8 H. Ohno, *Electrochemical Aspects of Ionic Liquids*, Wiley-Interscience, Hoboken, 2011.
9 A. B. H. Susan, T. Kaneko, A. Noda and M. Watanabe, *J. Am. Chem. Soc.*, 2005, **127**, 4976.
10 M. A. Néouze, J. L. Bideau, P. Gaveau, S. Bellayer and A. Vioux, *Chem. Mater.*, 2006, **18**(17), 3931.
11 W. Kubo, K. Murakoshi, T. Kitamura, S. Yoshida, M. Haruki, K. Hanabusa, H. Shirai, Y. Wada and S. Yanagida, *J. Phys. Chem. B*, 2001, **105**, 12809–12815.
12 T. Fukushima, A. Kosaka, Y. Ishimura, T. Yamamoto, T. Takigawa, N. Ishii and T. Aida, *Science*, 2003, **300**, 2072.
13 K. Ueno, K. Hata, T. Katakabe, M. Kondoh and M. Watanabe, *J. Phys. Chem. B*, 2008, **112**, 9013.
14 K. Ueno, S. Imaizumi, K. Hata and M. Watanabe, *Langmuir*, 2009, **25**, 825.
15 R. Marcillla, F. Alcaide, H. Sardon, J. A. Pomposo, C. Pozo-Gonzalo and D. Mecerreyes, *Electrochem. Commun.*, 2006, **8**, 482.
16 M. G. Kang, K. S. Ryu, S. H. Chang and N. G. Park, *ETRI J.*, 2004, **26**(6), 647.
17 B. Orel, A. Šurca Vuk, V. Jovanovski, R. Ješe, L. Slemenik Perše, S. B. Hočevar, E. A. Hutton, B. Ogorevc and A. Jesih, *Electrochem. Commun.*, 2005, **7**, 692.
18 V. Jovanovski, B. Orel, R. Ješe, A. Šurca Vuk, G. Mali, S. B. Hočevar, J. Grdadolnik, E. Stathatos and P. Lianos, *J. Phys. Chem. B*, 2005, **109**, 14347.
19 B. Orel, R. Ješe, A. Šurca Vuk, V. Jovanovski, L. Slemenik Perše and M. Žumer, *J. Nanosci. Nanotechnol.*, 2006, **6**, 1.
20 E. Stathatos, V. Jovanovski, B. Orel, I. Jerman and P. Lianos, *J. Phys. Chem. C*, 2007, **111**, 6528.
21 J. P. Lee, B. Yoo, T. Suresh, M. S. Kang, R. Vital and K. J. Kim, *Electrochim. Acta*, 2009, **54**, 4365.
22 M. Wang, X. Xiao, X. Zhou, X. Li and Y. Lin, *Sol. Energy Mater. Sol. Cells*, 2007, **91**, 785.
23 A. Fukui, R. Komiya, R. Yamanaka, A. Islam and L. Han, *Sol. Energy Mater. Sol. Cells*, 2006, **90**, 649.
24 H. Wang, X. Liu, Z. Wang, H. Li and D. Li, *J. Phys. Chem. B*, 2006, **110**, 5970.
25 B. Orel, R. Ješe, A. Vilčnik and U. Lavrenčič Štangar, *J. Sol-Gel Sci. Technol.*, 2005, **34**, 251.
26 C. A. Fyfe and P. P. Aroca, *J. Phys. Chem. B*, 1997, **101**, 9504.
27 H. H. Winter and F. Chambon, *J. Rheol.*, 1986, **30**, 367.
28 H. H. Winter and M. Mours, *Adv. Polym. Sci.*, 1997, **134**, 165.
29 G. M. Kavanagh and S. B. Ross-Murphy, *Prog. Polym. Sci.*, 1998, **23**, 533.
30 E. R. Payro and J. L. Llacuna, *J. Non-Cryst. Solids*, 2006, **352**, 2220.
31 M. Jokinen, E. Györvary and J. B. Rosenholm, *Colloids Surf., A*, 1998, **141**, 205.
32 V. H. V. Sarmento, K. Dahmouche, C. V. Santili and S. H. Pulcinelli, *J. Non-Cryst. Solids*, 2002, **304**, 134.
33 M. G. McLin and C. A. Angell, *J. Phys. Chem.*, 1991, **95**, 9464.
34 M. G. McLin and C. A. Angell, *Polymer*, 1996, **37**, 4713.
35 M. L. P. Le, F. Alloin, P. Strobel, J. C. Lepretre, C. P. Del Valle and P. Judeinstein, *J. Phys. Chem. B*, 2010, **114**, 894.
36 M. L. P. Le, L. Cointeaux, P. Strobel, J. C. Lepretre, P. Judeinstein and F. Alloin, *J. Phys. Chem. C*, 2012, **116**, 7712.
37 M. Gorlov, H. Pettersson, A. Hagfeldt and L. Kloo, *Inorg. Chem.*, 2007, **46**, 3566.
38 P. Wachter, M. Zistler, C. Schreiner, M. Berginc, U. Opara Krašovec, D. Gerhard, P. Wasserscheid, A. Hinsch, H. J. Gores and J. Photochem, *J. Photochem. Photobiol., A*, 2008, **197**, 25.
39 A. Šurca Vuk, M. Gaberšček, B. Orel and P. Colomban, *J. Electrochem. Soc.*, 2004, **151**, E150.
40 P. G. Gottschalk and J. R. Dunn, *Anal. Biochem.*, 2005, **343**, 54.
41 M. Čolović, Ph.D. thesis, Ljubljana, 2012.
42 N. E. Heimer, R. E. Del Sesto, Z. Meng, J. S. Wilkes and W. R. Carper, *J. Mol. Liq.*, 2006, **124**, 84.
43 E. R. Talaty, S. Raja, V. J. Storhaug, A. Dölle and W. R. Carper, *J. Phys. Chem. B*, 2004, **108**, 13177.
44 K. G. Sharp, *J. Sol-Gel Sci. Technol.*, 1994, **2**, 35.
45 R. G. Larson, *The Structure and Rheology of Complex Fluids*, Oxford University Press, New York, 1999.
46 R. Lapasin and S. Pricl, *Rheology of Industrial Polysaccharides: Theory and Applications*, Blackie Academic & Professional, London, 1995.
47 F. Chambon, Z. S. Petrovic, W. J. MacKnight and H. H. Winter, *Macromolecules*, 1986, **19**, 2146.
48 T. G. Metzger, *The Rheology Handbook*, Vincentz Network, Hannover, 2nd edn, 2006.